Spherical-Harmonic Approximation to the Forward Problem of Electrocardiology

R. Martin Arthur, PhD

***Abstract*— Forward-problem solutions were approximated using spherical-harmonic series on an adult-male torso model with heart and lungs. These approximations were found using only a knowledge of torso-model geometry and were not based on a prior solution for surface potentials. Because these series depend only on polar and azimuthal angles, they allow continuous estimation of the forward problem solution over the torso without further knowledge of the torso geometry. Compared to the conventional method, potentials estimated from fifth-degree series for eight distributed double-layer sources had an average relative error (RE) of 0.036. REs were similar with and without torso inhomogeneities. The fifth-degree series solution (36 terms) was found four times faster than the conventional method and provided a data reduction factor of about 20 in the 715-node torso model studied. Spherical-harmonic series transform surface potentials into an orthogonal basis set whose spatial-frequency content increases with increasing degree. Consequently, these series may provide a structure for the systematic study of the effect on forward-problem solutions of both changes in torso shape and inclusion of inhomogeneities.**

***Index Terms*— Cardiac sources, forward problem, spherical harmonics, torso model**

I. Introduction

Numerical methods for solving the far-field forward problem of electrocardiology in realistic torso models are well known. These techniques are based on Maxwell's equations which have been simplified because propagation, capacitive, and inductive effects can be neglected in the human body at frequencies observed in cardiac sources [1]. One of the most commonly employed forward-problem techniques is based on an integral formulation in which potentials are found directly at each surface element due to a given source in or on the heart [2], [3], [4].

Using the integral formulation, torso-surface potentials are often found iteratively [1], [5], [6]. Typically, the initial values for the surface potentials are those of the cardiac source of interest in an infinite medium. Convergence of the conventional, iterative process yields the bounded-medium potential at each of the discrete elements of the torso model. Forward-problem results can be used to specify transfer coefficients for use in inverse solutions, which are aimed at finding cardiac-equivalent generators. If the sites of the forward-problem solutions do not coincide with electrocardiographic measurement sites, however, then transfer coefficients must be interpolated to find values at the electrode locations.

In this study the polar- and azimuthal-angle solutions for Laplace's equation in spherical coordinates, namely spherical harmonics, were used as the basis functions for a series approximation to forward-problem solutions [7], [8], [9]. These spherical-harmonic series can be found without prior knowledge of the conventional, iterative solution. Approximating forward-problem solutions with spherical harmonics allows a list of potentials at discrete torso sites to be replaced with a smaller set of coefficients from which the forward-problem solution can be calculated everywhere on the torso surface. Thus, only the azimuthal and polar angles at a site of interest are needed to estimate the forward-problem solution there. Furthermore, spherical-harmonic decomposition of the forward problem may offer a suitable structure in which to systematically study the influence of torso shape and inhomogeneities on torso potentials.

For this study, spherical-harmonic series were constructed to approximate forward-problem solutions for both uniform, double-layer sources and orthogonal, dipole and quadrupole sources in an inhomogeneous, adult-male torso. Both distributed and discrete sources were used because any set of distributed sources is arbitrary and necessarily incomplete. Discrete multipolar sources, however, can be combined to characterize any distributed source. The quality of the spherical-harmonic series was characterized by comparison to conventional, iterative solutions. Spherical-harmonic series were also examined for: 1) reduction in computation time, 2) data reduction in representation, 3) use in interpolation, and 4) spatial-frequency decomposition of surface potentials.

II. Forward-Problem Solution on the Surface of an Inhomogeneous Torso

The integral solution to potential distribution $V(\mathbf{r})$ on the surface of an inhomogeneous conductor in an insulating medium (air) due to an internal source $\mathbf{J}^i$ is given by [1], [2], [3].

$$\begin{aligned} V(\mathbf{r}) &= \frac{1}{2\pi(\sigma_r^- + \sigma_r^+)} \left[\int_v \mathbf{J}^i \cdot \nabla \left(\frac{1}{r'}\right) \, dv \right. \\ &- \left. \sum_{s=1}^{m} (\sigma_s^- - \sigma_s^+) \int_{S_s, r \neq r'} V(\mathbf{r}') \nabla \left(\frac{1}{r'}\right) \cdot d\mathbf{S} \right], \end{aligned} \tag{1}$$

where $\mathbf{r}'$ is the position vector to volume element of integration dv. The integral over volume v is the potential due to the source in an infinite medium. The surface integral excludes the point at which $V(\mathbf{r})$ is determined.

A. Torso Model

The torso model used in this study was a version of an adult-male model reported previously [6], with heart and lungs added. Figure 1 shows the node locations of the inhomogeneous torso model. The torso surface contained 715

R. M. Arthur is with the Department of Electrical Engineering, Washington University in St Louis. E-mail: rma@ee.wustl.edu

nodes in 23 contours of 31 nodes plus two caps. The heart surface, estimated from x-ray silhouettes of the subject of the torso study, contained 58 nodes in 7 contours of 8 nodes plus two caps. Each lung surface, taken from computerized-tomographic scans of an adult male, contained 110 nodes in 9 contours of 12 nodes plus two caps. Conductivity of the torso, heart and lungs was set to 0.2, 0.6, and 0.05 S/m, respectively [4]b,[10].

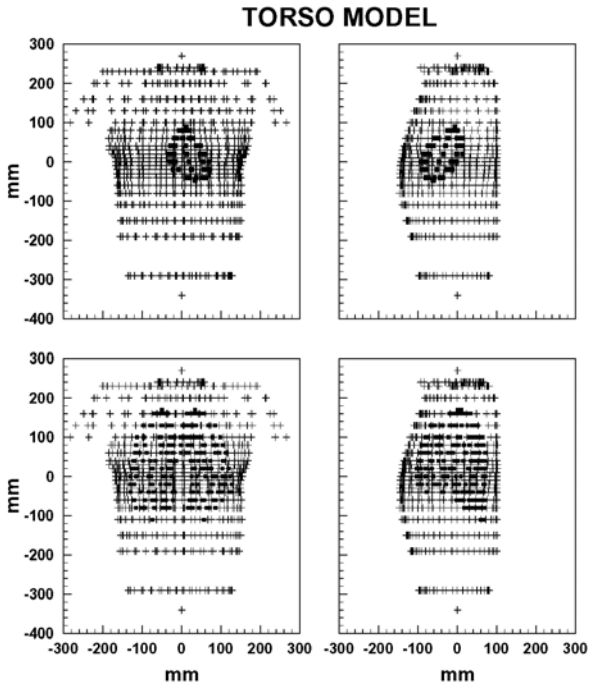

Fig. 1. Node locations of the surface elements of the inhomogeneous torso model. The torso surface, which had 715 nodes, contained a 58-node heart (upper panels) and 110-node lungs (lower panels). Conductivity of the torso, heart and lungs was 0.2, 0.6, and 0.05 S/m, respectively.

B. Discrete Forward-Problem Solutions

In matrix notation the discrete analog to eq. 1 for $V(\mathbf{r})$ in a torso model with heart and lungs is [1], [5]:

$$\begin{bmatrix} V_t \\ V_h \\ V_l \end{bmatrix} = \begin{bmatrix} \Omega_{tt} & \frac{(\sigma_h-\sigma_t)\Omega_{th}}{\sigma_t} & \frac{(\sigma_l-\sigma_t)\Omega_{tl}}{\sigma_t} \\ \frac{\sigma_t\Omega_{ht}}{\sigma_h+\sigma_t} & \frac{(\sigma_h-\sigma_t)\Omega_{hh}}{\sigma_h+\sigma_t} & \frac{(\sigma_l-\sigma_t)\Omega_{hl}}{\sigma_h+\sigma_t} \\ \frac{\sigma_t\Omega_{lt}}{\sigma_l+\sigma_t} & \frac{(\sigma_h-\sigma_t)\Omega_{lh}}{\sigma_l+\sigma_t} & \frac{(\sigma_l-\sigma_t)\Omega_{ll}}{\sigma_l+\sigma_t} \end{bmatrix} \begin{bmatrix} V_t \\ V_h \\ V_l \end{bmatrix} + 2 \begin{bmatrix} \frac{\Psi_t}{\sigma_t} \\ \frac{\Psi_h}{\sigma_h+\sigma_t} \\ \frac{\Psi_l}{\sigma_l+\sigma_t} \end{bmatrix} \quad (2)$$

where the subscripts t, h, and l designate the torso, heart, and lung, respectively. Ω is solid angle, σ is conductivity, and Ψ is infinite-medium potential.

The infinite-medium potential may be due to any source. Here we consider both distributed and discrete sources. The infinite-medium potential due to a double layer is [4]c:

$$\Psi^L(\mathbf{r}) = \frac{1}{4\pi\sigma}\int p \; d\Omega \quad , \quad (3)$$

where p is double-layer strength and $d\Omega$ is the solid angle it subtends. The infinite-medium potential due to a multipole source through order N (N=2 is a dipole) is [9]

$$\begin{aligned} \Psi^N(\mathbf{r}) &= \Psi^N(r,\theta,\phi) \\ &= \tfrac{1}{4\pi\sigma r}\sum_{n=1}^{N}\sum_{m=0}^{n}\left(\tfrac{1}{r}\right)^n P_n^m(\cos\theta) \\ &\times \left[a_{nm}\cos(m\phi)+b_{nm}\sin(m\phi)\right] \quad , \end{aligned} \quad (4)$$

where $P_n^m(\cos\theta)$ is an associated Legendre polynomial of degree n and order m [7], [8], [9]. For both distributed and discrete sources, infinite-medium potentials were evaluated using a 7-point numerical integral over each triangular surface element [11]. Solid angles were calculated using the method of Barnard and coworkers [5] as implemented by van Oosterom and Strackee [12]. The solid-angle matrix was deflated to remove its singularity [1], [13], [14].

Forward-problem solutions were found in the inhomogeneous torso model for eight uniform, double-layer sources. A -1 ma/mm double-layer source of radius 32 mm was located at a position corresponding to the x-ray center of the heart, which was at (20,0) in the frontal plane and (-50,0) in the sagittal plane. The double layer was aimed in five directions: 1) -Z (back-to-front), 2) X (right-to-left), 3) midway between -Z and Y, 4) midway between X and Y, and towards the apex of the heart. The double-layer disk was also moved towards the apex of the heart along the heart axis at distances of 10, 19, and 29 mm from the heart center, where its radius was reduced to 30, 26, and 14 mm, respectively. The forward-problem solution for each of the disks is the same as any double-layer configuration which forms a closed double-layer surface with the disk, so that the solution for each disk is the same as that for an infinite number of complementary double-layer sources [4]c. Forward-problem solutions were also found for unit-dipole and quadrupole sources. Discrete unit sources were located at the heart center.

Torso-surface potentials were found for the eight distributed sources and for the eight discrete sources by iterating eq. 2. For both sets of sources the maximum ratio of RMS value of the change in potential to the RMS value of the potential for the set of sources reached -60 dB after 17 iterations. Torso-surface potentials for three of the distributed sources are shown in Figure 2.

III. Spherical-Harmonic Approximation to the Forward Problem

The infinite-medium potentials for the discrete primary sources in the forward problem, eq. 4, are described by terms in polar angle θ and azimuthal angle ϕ. These terms are unnormalized spherical harmonics [7], [8], [9]. In addition to the primary sources, whether distributed or discrete, secondary sources are established on the torso-model surfaces to meet boundary conditions [1], [4]a. The potentials of both primary and secondary sources may be described in terms of spherical harmonics, which allow continuous reconstruction of potentials over the torso-model surfaces. Spherical harmonics are a suitable choice as basis functions for describing the

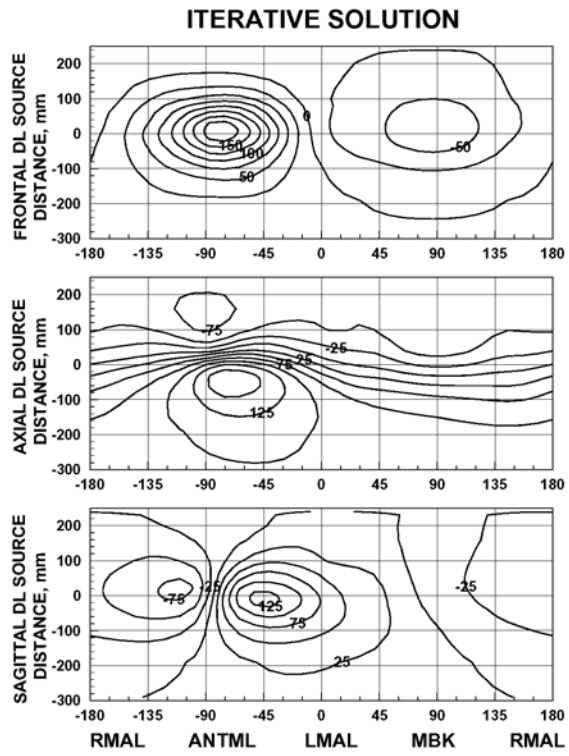

Fig. 2. Conventional, iterative solution to the body-surface potentials in the inhomogeneous torso. The source was a uniform double-layer of radius 32 mm located at the heart center. Its strength was 1 ma/mm. It was directed from back-to-front (upper panel), towards the apex of the heart (middle panel), and from right-to-left (lower panel). Equipotentials are given in millivolts.

bounded-medium potentials $V(\mathbf{r})$ due to the combined effects of primary and secondary sources, if the surface is single-value function of angle θ and ϕ and if the harmonic series furnish an efficient representation of surface potentials.

A finite-series approximation to $V(\mathbf{r})$ in terms of normalized spherical harmonics is given by:

$$V(r,\theta,\phi) = \sum_{n=0}^{N}\sum_{m=0}^{n} a_{nm}Y_{nm}^{e}(\theta,\phi) + b_{nm}Y_{nm}^{o}(\theta,\phi) \quad , \quad (5)$$

where

$$Y_{nm}^{e}(\theta,\phi) = \sqrt{\frac{2n+1}{4\pi}\frac{(n-m)!}{(n+m)!}}P_n^m(\cos\theta)\cos(m\phi) \quad , \quad (6)$$

and

$$Y_{nm}^{o}(\theta,\phi) = \sqrt{\frac{2n+1}{4\pi}\frac{(n-m)!}{(n+m)!}}P_n^m(\cos\theta)\sin(m\phi) \quad . \quad (7)$$

In matrix notation the spherical-harmonic approximation to $V(\mathbf{r})$ of eq. 5 is

$$[V] = [Y_{nm}^{e}Y_{nm}^{o}] \begin{bmatrix} a_{nm} \\ b_{nm} \end{bmatrix} \quad . \quad (8)$$

where the matrix containing $asubnm$ and $bsubnm$ is a column vector.

A. Solid-Angle , Spherical-Harmonic (SASH) Series

A spherical-harmonic approximation to $V(\mathbf{r})$ was found by substituting the matrix form of the approximation given by eq. 8, into the conventional, iterative solution to $V(\mathbf{r})$ (eq. 2). The resulting spherical-harmonic coefficients were designated a_{nm}^{sa} and b_{nm}^{sa}. They depend only on the infinite-medium potential for the source and the solid-angle matrix for the torso surfaces. These approximations to the forward problem were designated as solid-angle, spherical harmonic or SASH series. Although the torso-surface potentials were approximated, knowledge of conventional forward-problem solutions was not used to generate the SASH series.

Simplifying the matrix notation of eq. 2 for convenience:

$$[V] = [A][V] + [G] \quad , \quad (9)$$

or

$$([I] - [A])[V] = [G] \quad , \quad (10)$$

and substituting eq. 8 for [V] yields

$$([I] - [A])[Y_{nm}^{e}Y_{nm}^{o}] \begin{bmatrix} a_{nm}^{sa} \\ b_{nm}^{sa} \end{bmatrix} = [G] \quad , \quad (11)$$

where $[I]$ is the identity matrix. With $[H] = ([I] - [A])$ $[Y_{nm}^{e}Y_{nm}^{o}]$, eq. 11 becomes

$$[H] \begin{bmatrix} a_{nm}^{sa} \\ b_{nm}^{sa} \end{bmatrix} = [G] \quad . \quad (12)$$

Solving for a_{nm}^{sa} and b_{nm}^{sa} to minimize the mean-square error of the approximation gives the result that

$$\begin{bmatrix} a_{nm}^{sa} \\ b_{nm}^{sa} \end{bmatrix} = ([H]^t[H])^{-1}[H]^t[G] \quad . \quad (13)$$

Torso-surface potentials predicted by fifth-degree SASH series, which was based only on the infinite-medium potentials and the solid-angle matrix, are shown in Figure 3 for the same three double-layer sources depicted in Figure 2. The SASH-series maps of Figure 3 are difficult to distinguish from the iterative-solution maps of Figure 2 except in the region of the shoulders. As part of the quantitative evaluations of the SASH series, the SASH series were compared to series solutions which resulted from least-squares-error fits of the conventional forward-problem solutions. This comparison determined how close the SASH series were to spherical-harmonic coefficients found in the least-squares-error sense.

B. Least-Squares-Error (LSE) Series

The SASH approximations to the torso-surface potentials presented in Figure 3 did not use a knowledge of the conventional forward-problem solutions. If the conventional forward-problem solutions $V(\mathbf{r})$ are known, then they can also be matched on a least-squares-error (LSE) basis using a spherical-harmonic approximation.

The fit of the conventional, iterative solutions yields a set of spherical-harmonic coefficients, a_{nm}^{ls} and b_{nm}^{ls}. If

$$[Y_{nm}^{e}Y_{nm}^{o}] \begin{bmatrix} a_{nm}^{ls} \\ b_{nm}^{ls} \end{bmatrix} = [V] \quad . \quad (14)$$

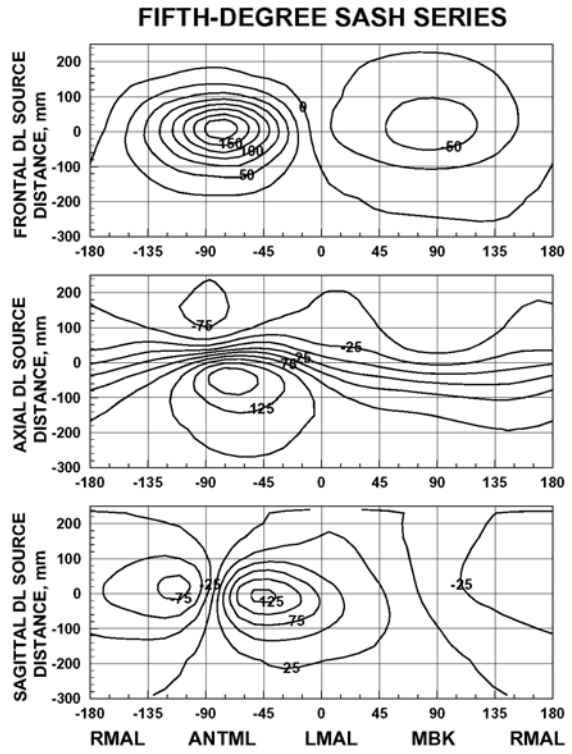

Fig. 3. Fifth-degree, spherical-harmonic series approximation to the body-surface potentials in the inhomogeneous torso. Series coefficients were determined from the solid-angle matrix for the torso and the infinite-medium potentials. The conventional forward-problem solution was not used in determining the solid-angle, spherical-harmonic (SASH) series. Sources were the same as those in the previous figure, namely a 32 mm, 1 ma/mm double-layer directed from back-to-front (upper panel), towards the apex of the heart (middle panel), and from right-to-left (lower panel). Equipotentials are given in millivolts.

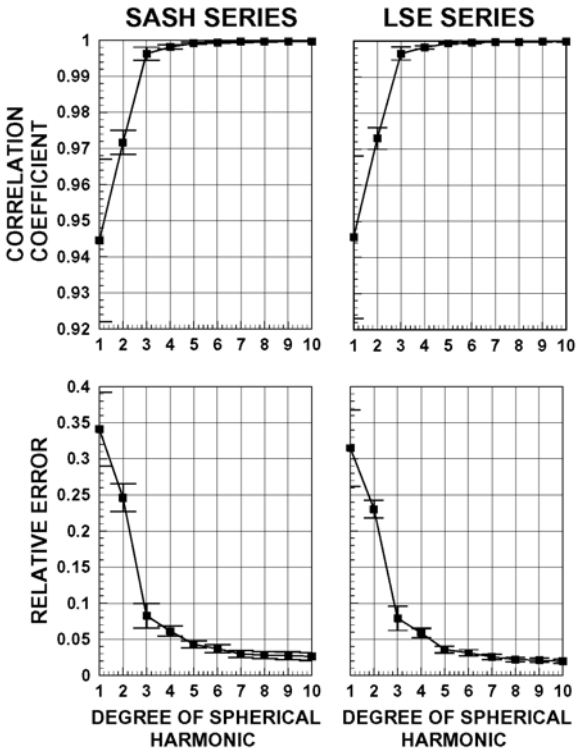

Fig. 4. Performance of the solid-angle (SASH) and least-squares-error (LSE) spherical harmonic approximations to the torso-surface potentials for double-layer sources. The mean and standard deviation of correlation coefficients and relative errors are shown for eight sources. Series approximations were compared to the conventional, iterative solution in each case. The SASH series, calculated without knowledge of the conventional solution, behaved almost identically to the LSE series, which was a fit of the conventional solution. Both series approximations appear to have reached an asymptote by about the fifth harmonic.

then

$$\begin{bmatrix} a_{nm}^{ls} \\ b_{nm}^{ls} \end{bmatrix} = ([Y_{nm}^{e} \quad Y_{nm}^{o}]^{t}[Y_{nm}^{e} Y_{nm}^{o}])^{-1}[Y_{nm}^{e} \quad Y_{nm}^{o}]^{t}[V] \quad . \tag{15}$$

Quantitative evaluations were performed on both SASH series and LSE series as described in the next section.

IV. Evaluation of the Spherical-Harmonic Approximation

Torso-surface potentials on the inhomogeneous torso model predicted by first- through tenth-degree SASH and LSE series were compared to the conventional forward-problem solutions for the eight distributed sources using two measures as shown in Figure 4. Comparison were evaluated using the correlation coefficient and relative error [15], whose mean and standard deviation are shown for the eight sources. Note that the SASH series, calculated without knowledge of the conventional solution, behaved almost identically to the LSE series, which was a fit of the conventional solution. Most of the improvement in the performance of either series approximation, with increasing degree of the approximation, occurred around the fifth to the seventh degree. Potentials calculated from fifth-degree SASH series for all eight sources had an average correlation coefficient and relative error of 0.9993 and 0.036, respectively. Average values for those measures for tenth-degree SASH series were 0.9997 and 0.026, respectively. Average values for the same measures for tenth-degree LSE series were 0.9998 and 0.020, respectively.

Results presented so far apply to forward-problem solutions on the torso surface. Approximations can be found, however, on all surfaces of the torso model. Furthermore, approximations can be found for potentials due to secondary sources, as well as for the total potentials. Table I presents the mean and standard deviation for fifth- and seventh-degree LSE approximation on all four surfaces in the torso model for both total and secondary-source potentials. Note that for each surface the overall quality of the approximation for total compared to secondary sources was similar. The degree of the approximation can vary with each surface depending on the accuracy desired and the number of nodes used. Because the lungs were not single-valued functions of θ and ϕ, infinite-medium potentials (eq. 4) were used instead of spherical harmonics (eqs. 6 and 7) to define the basis functions. The difference between the two basis sets is that radius is required to calculate the approximation from the infinite-medium potentials. In other words, the geometry of the lungs is needed to

map the approximation values. In contrast, the geometry of the torso and heart is not needed to map the spherical-harmonic approximation to forward-problem solutions.

TABLE I
PERFORMANCE MEASURES FOR UNIFORM DOUBLE-LAYER SOURCES
FIFTH- AND SEVENTH-DEGREE APPROXIMATIONS IN THE
INHOMOGENEOUS TORSO

Total Pot.	Torso	Heart	Right Lung[1]	Left Lung[1]
CC (n=5)	$.9993 \pm .0002$	$.9987 \pm .0010$	$.9973 \pm .0006$	$.9976 \pm .0006$
CC (n=7)	$.9997 \pm .0001$	$.9999 \pm .0001$	$.9994 \pm .0001$	$.9990 \pm .0002$
RE (n=5)	$.036 \pm .006$	$.049 \pm .018$	$.074 \pm .009$	$.069 \pm .009$
RE (n=7)	$.026 \pm .004$	$.016 \pm .005$	$.034 \pm .004$	$.043 \pm .005$
Sec. Pot.	Torso	Heart	Right Lung[1]	Left Lung[1]
CC (n=5)	$.9981 \pm .0001$	$.9999 \pm .0002$	$.9972 \pm .0006$	$.9975 \pm .0008$
CC (n=7)	$.9991 \pm .0002$	$1.0000 \pm .0001$	$.9994 \pm .0001$	$.9991 \pm .0002$
RE (n=5)	$.062 \pm .006$	$.011 \pm .004$	$.074 \pm .009$	$.069 \pm .012$
RE (n=7)	$.042 \pm .005$	$.006 \pm .002$	$.033 \pm .005$	$.042 \pm .006$

1) Match using Infinite-medium potentials

TABLE II
PERFORMANCE MEASURES FOR DIPOLE AND QUADRUPOLE SOURCES
FIFTH- AND SEVENTH-DEGREE APPROXIMATIONS IN THE
INHOMOGENEOUS TORSO

Dip. Pot.	Torso	Heart	Right Lung[1]	Left Lung[1]
CC (n=5)	$.9993 \pm .0003$	$.9997 \pm .0000$	$.9976 \pm .0009$	$.9980 \pm .0003$
CC (n=7)	$.9996 \pm .0002$	$.9999 \pm .0000$	$.9995 \pm .0001$	$.9992 \pm .0003$
RE (n=5)	$.038 \pm .007$	$.022 \pm .002$	$.068 \pm .013$	$.063 \pm .005$
RE (n=7)	$.028 \pm .006$	$.014 \pm .001$	$.030 \pm .005$	$.040 \pm .007$
Quad. Pot.	Torso	Heart	Right Lung[1]	Left Lung[1]
CC (n=5)	$.9959 \pm .0012$	$.9995 \pm .0001$	$.9985 \pm .0005$	$.9970 \pm .0013$
CC (n=7)	$.9991 \pm .0001$	$.9998 \pm .0000$	$.9997 \pm .0000$	$.9990 \pm .0003$
RE (n=5)	$.089 \pm .013$	$.031 \pm .002$	$.055 \pm .010$	$.077 \pm .016$
RE (n=7)	$.041 \pm .004$	$.017 \pm .003$	$.026 \pm .001$	$.044 \pm .007$

1) Match using Infinite-medium potentials

The results in Table I summarize the performance of eight uniformly distributed sources. Obviously, many other distributed sources could have been studied. Multipolar sources, however, can be combined to characterize any distributed source. Table II presents the mean and standard deviation for fifth- and seventh-degree LSE approximation on all four surfaces in the torso model to the total potentials of the three dipolar and five quadrupolar orthogonal sources. Note that for each surface the quality of the approximation to the total potential for the fixed, discrete dipolar sources was comparable to that for the double-layer sources (Table I). For example, there is no significant difference on any surface between the relative errors for the distributed and dipolar sources. The performance for the quadrupolar sources is also similar to that for the dipolar sources.

V. DISCUSSION

Although the methods for generating the direct and least-squares-error approximations to the forward problem can be applied with other basis functions, spherical harmonics were successful in characterizing forward-problem solutions for a variety of distributed and discrete sources. The average relative error for seventh-degree, spherical-harmonic series over the torso and heart in the four-surface, torso model was 0.024 for the 48 potential maps described in Tables I and II. The characteristics of these sources suggest that these results are representative of many other source configurations. Each of the eight uniform double-layer sources actually represents an infinite number of sources because the forward-problem solution is the same for any double layer that closes the surface containing the double-layer disks that were used [4]. Furthermore, the dipole and quadrupole sources are the first terms in a multipole expansion which can be used to represent any arbitrary source. Therefore, similar relative errors can be expected for a wide variety of other possible sources. Similar relative errors are also expected for additional inhomogeneities because errors were virtually unchanged as inhomogeneities were added to the torso model. The average relative errors of the seventh-degree, spherical-harmonic series for the total potential due to the eight distributed sources on the torso surface were 0.026, 0.025, and 0.026 for the homogeneous torso, for the torso with heart, and for the torso with heart and lungs, respectively. Spherical-harmonic series also had comparable relative errors when used to match the transfer coefficients that relate epicardial to torso-surface potentials [16]. Transfer coefficients for a 58-node heart in a 715-node torso were matched with relative errors of 0.065, 0.037, and 0.026 for fifth-, seventh-, and tenth-degree series, respectively.

Spherical-harmonic approximations succeeded in matching forward-problem solutions on the torso and heart. These surfaces were single-valued functions of the polar and azimuthal angles from an origin at the x-ray center of the heart. The lungs, of course, were not. Unfortunately, moving the origin for the spherical-harmonic approximation to the center of the lungs did not provide a comparable fit to that on the torso or heart because the spherical-harmonic series was not located in the vicinity of the primary source. Infinite-medium-potential approximations at the x-ray heart center, however, did provide matches on the lungs which were comparable to the fits on the torso and heart found using spherical harmonics. Infinite-medium approximations are composed of a function of the radius in addition to spherical harmonics (Compare eq. 4 to eqs. 6 and 7). Although spherical harmonics provided a successful basis set for the torso and heart, other inhomogeneities like the lungs presumably will require basis functions that must incorporate knowledge of the geometry of the inhomogeneity to reconstruct forward-problem solutions.

Computation of both the SASH and LSE series required inversion of an NxN matrix, where N is the number of coefficients in the spherical-harmonic series. N is the degree of the harmonic plus one squared. Because N can be much smaller than the number of elements in the surface model, the forward problem can be approximated faster than the conventional, iterative solution can be found. Forming the SASH series was slower than the finding the LSE because it also required multiplying the basis functions by the solid-angle matrix. The SASH series was 3.8, 2.3, and 1.2 times faster than the conventional solution for fifth-, seventh-, and tenth-degree approximations. The LSE series was 76, 38, and 7 times faster than the conventional solution for fifth-, seventh-, and tenth-degree approximations.

Results of the forward-problem using the iterative, con-

ventional method are tabulated at nodes of the torso model. Representation of torso-surface potentials with a spherical-harmonic series replaces the list of potentials with a set of coefficients. Series representation of surface potentials has two advantages. First, the set of series coefficients can be smaller than the list of potentials. Although the list need not contain the potentials at all node, to include them all would require 715 values in this study because the torso model contained 715 nodes. A fifth-degree series contains 36 coefficients. Thus the number of items required to represent torso potentials using a fifth-degree series is reduced by a factor of about 20. The reduction is by a factor of 11 and 6 for seventh- and tenth-degree spherical harmonics, respectively. Second, the series can be used to predict surface potentials everywhere on the torso surface not just at the nodes of the torso model. This advantage may be useful for cases in which electrocardiographic measurements are made at sites which differ from the location of torso-model elements. Using the conventional approach, both the torso geometry and the forward-problem solution are required to interpolate the transfer coefficients to find the value at such an electrode site. With the spherical harmonics, only the location of the electrode, as specified by its polar angle θ and its azimuthal angle ϕ is needed; torso-model geometry is no longer needed.

The spherical-harmonic approximations are a transformation of surface potentials into an orthogonal basis set whose spatial-frequency content increases with increasing degree. Consequently, their use may provide a structure for the systematic study of the effects on forward-problem solutions of both changes in torso shape and inclusion of inhomogeneities. Consider Figure 5, which shows the relative contribution of each degree of a tenth-degree LSE series for the torso potentials in the torso model with and without inhomogeneities. The changes in the contributions to torso potentials are shown with respect to the values found in the homogeneous torso which was used as baseline. The homogeneous torso values were set to zero for all harmonics and the solutions with inhomogeneities adjusted accordingly. Clearly, the effect of the inhomogeneities depends on the degree of the harmonic and the amount of change at each harmonic depends on the nature of the source. For example, for all three sources the addition of the cardiac inhomogeneity reduced the contribution of the fourth harmonic by about 5 dB. When the lungs were added, however, the contribution for the fourth harmonic increased by 4 dB for the frontal source, decreased by 3 dB for the axial source, and was unchanged for the sagittal source.

VI. Conclusions

Low-degree, spherical-harmonic series provide an accurate representation of forward-problem solutions for both distributed and discrete cardiac sources. These series can be found more rapidly than the conventional, iterative solutions with or without knowledge of those solutions. Series coefficients furnish a more compact representation of surface potentials than a tabulated list of potentials at the elements of the torso model. Furthermore, the series yield continuous approximations of forward-problem solutions which are valid everywhere on the torso surface.

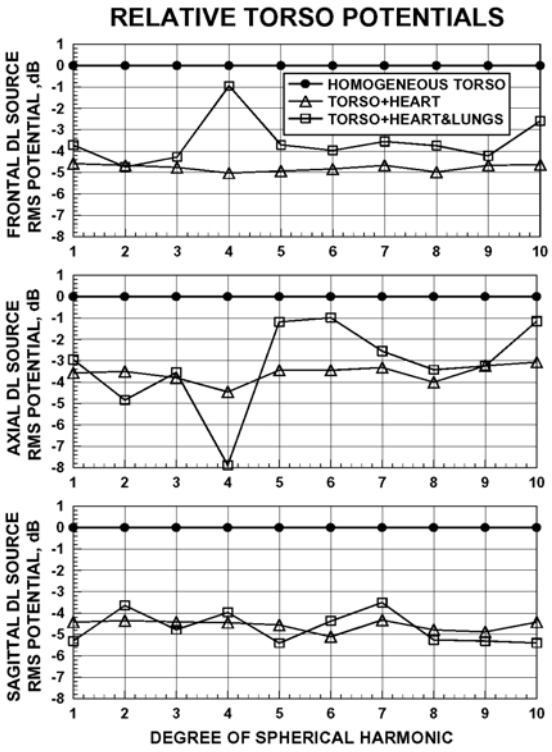

Fig. 5. Relative contribution of each degree of a tenth-degree LSE series for the torso potentials in the torso model with and without inhomogeneities. Changes in the contributions to torso potentials are shown with respect to the values found in the homogeneous torso which was used as baseline, i.e., set to zero. The effect of the inhomogeneities depends on the direction of the source and the spatial frequencies of the torso potentials, which increase with the degree of the spherical harmonic.

VII. Acknowledgements

This work was supported in part by Washington University.

References

[1] R. M. Gulrajani, F. A. Roberge, and G. E. Mailloux, "The forward problem of electrocardiography," in *Comprehensive Electrocardiology*, P. W. MacFarlane and T. D. Veitch Lawrie, Eds., vol. 1, pp. 197–235. Pergamon Press, 1989.

[2] R. C. Barr, T. C. Pilkington, J. P. Boineau, and M. S. Spach, "Determining surface potentials from current dipoles, with application to electrocardiography," *IEEE Trans. on Biomed. Engr.*, vol. BME-13, pp. 88–92, 1966.

[3] A. C. L. Barnard, I. M. Duck, and M. S. Lynn, "The application of electromagnetic theory to electrocardiology. i. Derivation of the integral equations," *Biophysical Journal*, vol. 7, pp. 443–462, 1967.

[4] J. Malmivuo and R. Plonsey, *Bioelectromagnetism*, Oxford University Press, New York, 1995, a) 134–136, b) 140–141, c) 187-190.

[5] A. C. L. Barnard, I. M. Duck, M. S. Lynn, and W. P. Timlake, "The application of electromagnetic theory to electrocardiography ii. Numerical solution to the integral equations," *Biophys. J.*, vol. 7, pp. 463–491, 1967.

[6] R. M. Arthur, D.B. Geselowitz, S.A. Briller, and R.F. Trost, "Quadrupole components of the human surface electrocardiogram," *American Heart Journal*, vol. 83, no. 5, pp. 663–677, May, 1972.

[7] P. M. Morse and H. Fesbach, *Methods of Theoretical Physics*, McGraw-Hill, New York, 1953.

[8] G. Arfken, *Mathematical Methods for Physicists*, Academic Press, New York, 1966.

[9] R. Plonsey, *Bioelectric Phenomena*, McGraw-Hill, St Louis, 1969.

[10] S. Rush, J. A. Abildskov, and R. McFee, "Resistivity of body tissues at low frequency," *Circ. Res.*, vol. XII, pp. 40–50, 1963.

[11] M. Abramowitz and I. A. Stegun, Eds., *Handbook of Mathematical Functions*, National Bureau of Standards Applied Mathematics Series. US Government Printing Office, Washington DC, 1968.
[12] A. Van Oosterom and J. Strackee, "The solid angle of a plane triangle," *IEEE Trans. on Biomed. Engr.*, vol. 30, no. 2, pp. 125–126, 1983.
[13] M. S. Lynn and W. P. Timlake, "The use of multiple deflations in the numerical solution of singular systems of equations, with applications to potential theory," *SIAM Journal of Numerical Analysis*, vol. 5, no. 2, pp. 303–322, 1968.
[14] M. S. Lynn and W. P. Timlake, "The numerical solution of singular integral equations of potential theory," *Numerical Mathematics*, vol. 11, pp. 77–98, 1968.
[15] P. R. Johnston and R. M. Gulrajani, "A new method for regularization parameter determination in the inverse problem of electrocardiography," *IEEE Trans. on Biomed. Engr.*, vol. 44, no. 1, pp. 19–39, 1997.
[16] R. C. Barr, III M. Ramsey, and M. S. Spach, "Relating epicardial to body surface potential distributions by means of transfer coefficients based on geometry measurements," *IEEE Transactions on Biomedical Engineering*, vol. BME-24, no. 1, pp. 1–11, 1977.